Available online at www.sciencedirect.com
SCIENCE DIRECT®
Biochimica et Biophysica Acta 1655 (2004) 37–44
BIOCHIMICA ET BIOPHYSICA ACTA
BBA
www.bba-direct.com

Review

Theory and simulation of proton-coupled electron transfer, hydrogen-atom transfer, and proton translocation in proteins

R.I. Cukier*

Department of Chemistry, Michigan State University, East Lansing, MI 48824-1322, USA

Received 11 March 2003; accepted 25 June 2003

This work is dedicated to the memory of Gerald T. Babcock, a superb scientist, colleague, and friend

Abstract

A theory of proton coupled electron transfer (PCET) is reviewed with application to charge transfer steps in the photosystem II oxygen-evolving complex (PSII/OEC). The relation between PCET when it is a concerted electron proton transfer (ETPT) process and hydrogen-atom transfer (HAT) reactions is discussed. Signatures expected for HAT reactions in terms of the size of the kinetic isotope effect and overall magnitude of the rate constant are discussed in the context of PSII/OEC. The formal similarity of ETPT to proton transfer and translocation is used to introduce a combined quantum mechanical (for the transferring protons) and molecular dynamics for the heavy-atom degrees of freedom approach. The method is used to examine double proton transfer in cytochrome *c* oxidase where two waters and a glutamate (Glu286) that is implicated in the proton translocation mechanism form a cyclic hydrogen bonded structure. Protonation of the glutamate is found to occur in agreement with experimental results.

Keywords: Proton and electron transfer; Proton translocation; Photosystem II oxygen evolving complex; Cytcohrome *c* oxidase

1. Introduction

I had not appreciated how much Gerry influenced my choice of research problems until I sat down to write this review and found that I wanted to discuss aspects of electron, proton and hydrogen-atom transfer with application to the photosystem II oxygen-evolving complex (PSII OEC), and aspects of proton translocation with application to cytochrome *c* oxidase (CcO), two areas in which Gerry had a major impact [1,2]. Our last well-developed interactions were on the topic of the distinction between H-atom and coupled electron-proton transfer and its relevance to PSII OEC [3,4]. We had numerous discussions on the defining features of electron and proton transfer in condensed phases. How their transfer requires a quantum mechanical description of the electrons and/or protons and how these quantum degrees of freedom are coupled to an (often) classical medium that serves to provide the energetic fluctuations that drive the transfer. And how biological systems, as exemplified by proteins with their cofactors and bound waters, utilize the large energetics associated with electron-transfer (ET), proton-transfer (PT), proton-coupled electron-transfer (PCET), dissociative pcet (DPCET), and hydrogen-atom transfer (HAT) that, with the exception of hydrogen-atom transfer, typically involve large charge rearrangements with concomitant strong coupling to the surrounding medium [5,6]. In a related vein, a long-standing interest of mine is in understanding the mechanism of proton translocation in proteins. While Gerry was not able to see the application to cytochrome *c* oxidase discussed below, he followed with great interest my initial attempts to find a computationally efficient scheme to combine a quantum mechanical description of the protons involved in translocation coupled with a classical description of the medium that drives the proton translocation.

2. Photosystem II oxygen-evolving complex

It is a tribute to Gerry's intellectual curiosity and abilities that he was willing to put in the effort to understand the

* Fax: +1-517-353-1793.
E-mail address: cukier@cem.msu.edu (R.I. Cukier).

0005-2728/$ - see front matter © 2004 Elsevier B.V. All rights reserved.
doi:10.1016/j.bbabio.2003.06.011

theoretical ideas needed to characterize charge transfer reactions and then suggest appropriate biological systems for application. A system we devoted attention to consists of steps in the chain of charge-transfer reactions in the PSII/OEC, designated as Reaction 1 in Fig. 1 [1,7–13]. For a *consecutive* pathway, the reactions are

$$P680^{+} + Y_ZOH{-}NR_2 \overset{ET}{\rightarrow} P680 + [Y_ZOH{-}NR_2]^{\bullet +} \overset{PT}{\rightarrow} P680 + [Y_ZO{-}HNR_2]^{\bullet +}$$

As a *concerted* process, the reaction is

$$P680^{+} + Y_ZOH{-}NR_2 \xrightarrow{ETPT} P680 + [Y_ZOH - NR_2]^{\bullet +}.$$

In this scheme, a reaction center chlorophyll P680 has been previously oxidized to $P680^{+}$. The tryrosine, denoted as Y_ZOH, is oxidized to a tryrosyl radical and re-reduces $P680^{+}$ to P680. The proton in the tyrosyl-histidine (NR_2) hydrogen bond transfers from the phenol to the nitrogen of the base. The combination of ET to form the tyrosyl radical and PT from the phenol to the histidine comprises the PCET system. In a succeeding reaction, the tyrosyl radical formed can then be reduced in the S-state cycle that transfers a hydrogen atom from water bound to the Manganese cluster, as displayed in Fig. 1, Reaction 2. This scheme can be viewed as either consecutive reactions of ET/PT or PT/ET, or as a concerted, hydrogen-atom transfer $Y_ZO^{\bullet}/Mn(H_2O) \rightarrow Y_ZOH/Mn^{+}(OH^{-})$. We suggested [3] that the $Y_Z^{\bullet}$ reduction occurs by a concerted process.

A distinctive feature of the description of charge transfer reactions is the use of the Born–Oppenheimer separation to assert that the potential energy surface (pes) for the light particle (electron and/or proton) depends parametrically on the nuclear coordinates of the surrounding medium [14–16]. The quantum tunneling that transfers the light particle takes place when a medium thermal fluctuation symmetrizes the pes (resonance condition) for the light particle. If the symmetrization occurs as separate events for the electron and proton, we classify the process as a consecutive reaction mechanism of ET/PT or PT/ET. If the symmetrization occurs for the electron and proton simultaneously, we view it as a concerted ETPT reaction. Which pathway (ET/PT PT/

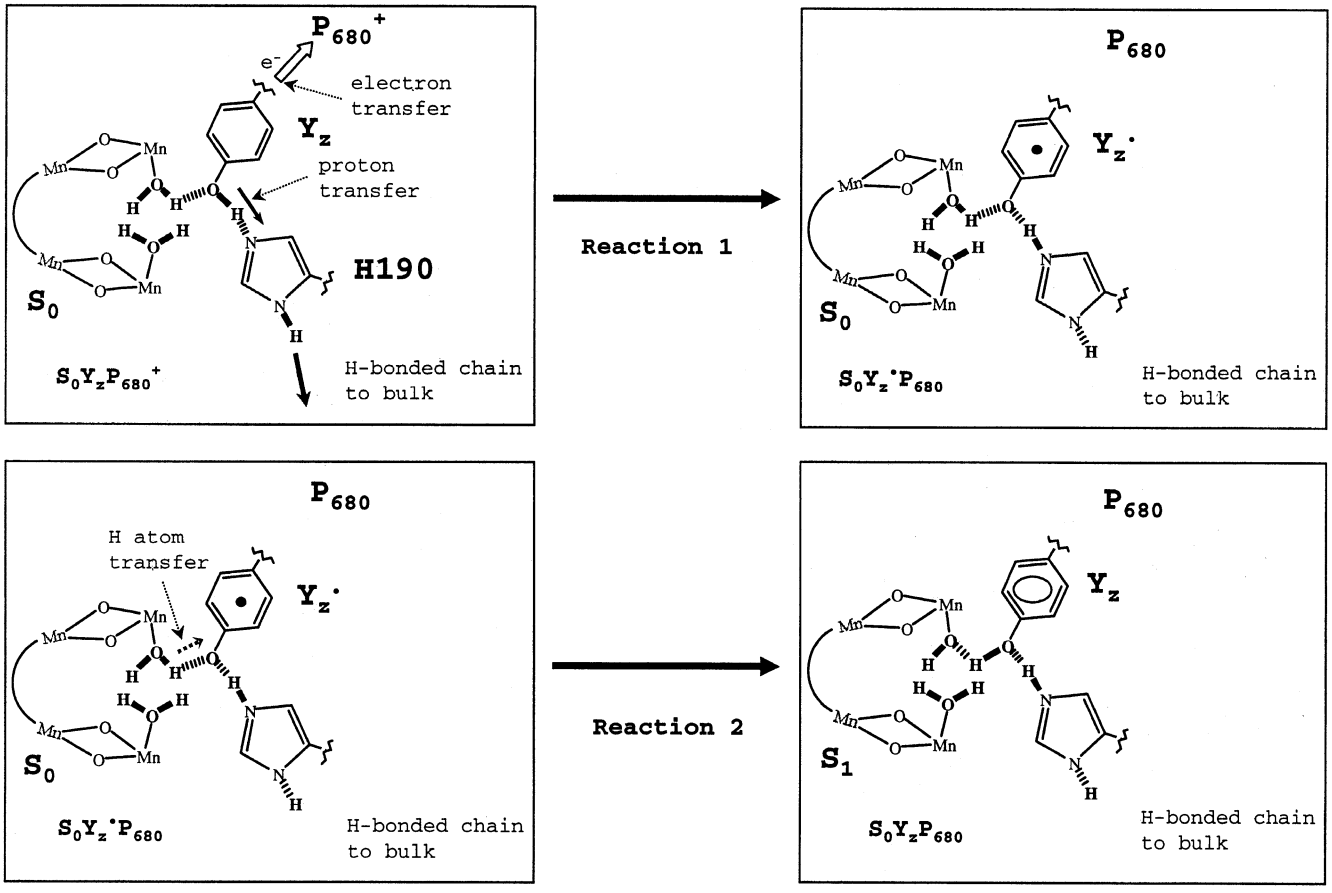

Fig. 1. Hydrogen atom abstraction model for photosynthetic water oxidation. The catalytic center of PSII is postulated to be arranged as drawn. Substrate water binds terminally to the Manganese ions within hydrogen bonding distance (. . . . . .) of the Y_Z phenol group. Open arrows show the flow of electrons and solid arrows the flow of protons for the oxidation of Y_Z (Reaction 1). Oxidation of Y_Z is considered to be a proton-coupled electron transfer reaction. The dotted arrow shows the H-atom transfer to $Y_Z^{\bullet}$, from the water bound to the $(Mn)_4$ cluster (Reaction 2). Reduction of $Y_Z^{\bullet}$ is considered to be a hydrogen-atom transfer reaction that may be summarized as $Y_ZO^{\bullet}/Mn(H_2O) \rightarrow Y_ZOH/Mn^{+}(OH^{-})$.

ET or ETPT) will dominate is an issue of competitive rates that will be determined by electronic structure effects of the reactants and products, as well as by the coupling of the electron's and proton's reactant and product state charge distributions to the surrounding medium [5,6]. A further distinction can be made relative to ETPT and HAT [17]. As indicated in Fig. 1, Reaction 1, the electron is perforce tunneling a long distance; and, consequently, the appropriate description is in terms of weak coupling between electron donor and acceptor (a nonadiabatic regime). For the proton, we may also assume that its transfer can be described by a weak coupling, nonadiabatic regime. Then, a PCET theory can be constructed, appropriate to both consecutive and concerted processes, using the assumed nonadiabatic behavior for electron and proton. A PCET theory when the electronic motion is adiabatic can also be constructed that we refer to as HAT. For HAT, the electron is transferring a relatively short distance (on the scale of a hydrogen-bond distance), as appropriate to Reaction 2 in Fig. 1, and its transfer should be considered as a strong coupling, adiabatic process. Indeed, in this situation, distinguishing a particular electron loses meaning and one electronic potential energy surface for the proton that simultaneously characterizes the electronic redistribution should suffice. The importance of the degree of adiabaticity to theories of ET, PT, PCET, and atom transfer in general was noted early on [14,18,19], and plays a prominent role in the PT approaches of Borgis and Staib [20] and Cukier and Zhu [21], and the PCET theories of Decornez and Hammes-Schiffer [22,23] and Georgievskii and Stuchebrukhov [24]. To construct a theory of HAT from this perspective we used [21] a Landau–Zener [25] approach that interpolates between the nonadiabatic (small coupling) and adiabatic (large coupling) limits.

A signature of the transition from concerted ETPT to HAT may be found in the magnitude of the kinetic isotope effect (KIE) [16,26]. We predicted that isotope effects may not be large, even though the transfer proceeds by tunneling. The effect arises from the dominance of adiabatic proton transfer when the configurations of the heavy-atom framework that surround the transferring group correspond to smaller-than-equilibrium heavy-atom distances, as first noted by Krishtalik [16]. For close heavy atom distances, the protonic potential surface has a low barrier, the splitting between the lowest states is large and, consequently, the adiabatic limit of the Landau–Zener expression that no longer distinguishes between the isotopes is appropriate. This leads to relatively small isotope effects, as has been found for a number of HAT reactions. Indeed, the simplest theory that can be written down has the form

$$k_{\mathrm{L}} = \int \mathrm{d}R_{\mathrm{AB}} P(R_{\mathrm{AB}}) k_{\mathrm{L}}^{\mathrm{LZ}}(R_{\mathrm{AB}}) \qquad (\mathrm{L} = \mathrm{H}, \mathrm{D}) \qquad (1)$$

where $P(R_{\mathrm{AB}})$ is the (isotope independent) thermal probability of observing the heavy-atom distance R_{AB} and $k_{\mathrm{L}}^{\mathrm{LZ}}(R_{AB})$ is the Landau–Zener-based rate constant for ETPT at the distance R_{AB}. In Fig. 2, we plot the integrand of Eq. (1) in a dimensionless form that shows the (modest) reduction in rate in going from proton to deuteron. If even shorter heavy atom distances are dominant the difference between the two curves is further reduced. For intramolecular hydrogen-atom transfers, using a typical pes for proton transfer, and heavy-atom masses and vibrational frequencies, isotope effects of $k_{\mathrm{H}}/k_{\mathrm{D}} \sim 1-6$ were found. For a bimolecular reaction, where the base and its corresponding acid must climb a repulsive wall to come close enough to react, $k_{\mathrm{H}}/k_{\mathrm{D}} \sim 1-20$. The results are quite sensitive to the details of the potential surface, and it must be stressed that the surfaces are rough approximations to the actual ones. Nevertheless, the prediction that isotope effects will be smaller than those based on equilibrium-distance transfers should be robust. A greater span in the KIE for a repulsive versus a bonded heavy atom potential surface is anticipated since there is more freedom in a non-bonded repulsive surface than in a bonded surface.

If a HAT reaction does exhibit a relatively small isotope effect (dominance by the strong-coupling, adiabatic regime), then the pre-exponential factor in the rate expression will be rather large, in contrast to the small value that would arise from electronic/protonic matrix elements that contribute to a nonadiabatic ETPT expression. If, in addition, the activation energy is small, predicted HAT rate constants will be large, because the adiabatic-limit prefactor is $\sim 10^{12}-10^{13}\ \mathrm{s}^{-1}$. Inclusion of inner-sphere vibrational contributions to the rate expression, appropriate for some HAT reactions, will lead to smaller rate constants, as found experimentally. Of course, with modest activation energies, the rates will already be in the range of observed values. For example, an activation energy of 7 kcal/mol will decrease the rate by five orders of magnitude relative to an activationless reaction. Even if the isotope effect in a

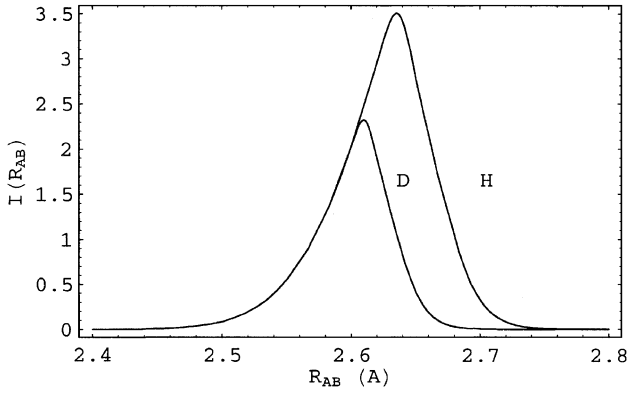

Fig. 2. $I_{\mathrm{L}}(R_{\mathrm{AB}})$ (L = H, D). The integrand in Eq. (1) plotted in dimensionless form. The D-curve is smaller than that for H, reflecting the smaller tunneling probability for D versus H for a given R_{AB} value. The rate constant is proportional to the areas under the curves, and the data show how modest isotope effects can result in HAT reactions.

HAT reaction is large, the pre-exponential factor can still be large because once the reaction is electronically adiabatic, the (small) electronic matrix element is absent from the rate constant expression. Thus, HAT reactions with large isotope effects can occur with respectable velocities.

Gerry was instrumental in using these ideas to rationalize the kinetic features of HAT reactions. The data on the reduction of $Y_Z^{\bullet}$ [1,27,28] when expressed in Arrhenius form, $k = A\exp(-E_a/kT)$, is characterized by a range of activation energies, $E_a \sim 1-9$ kcal/mol, small pre-exponential factors $A \sim 10^6-10^9$ s^{-1}, and small KIEs, $k_H/k_D \sim 1.3-2.9$. These ranges come from rate measurements particular to various S-state transitions and from different methods of sample preparation. $Y_Z^{\bullet}$ reduction is an excellent candidate for a HAT mechanism, in view of the geometry postulated in the Fig. 1, Reaction 2 scheme. A number of EPR, ENDOR and ESEEM-based studies [29–31] infer a Manganese to Y_Z tyrosine magnetic distance of around 6–8 Å. Recent crystal structures [32,33] indicate a distance of 7 Å from the center of the Manganese cluster to Y_Z. These distances can support a cluster composed of Manganese, a bound water and tyrosine in a geometric arrangement appropriate to a HAT reaction. Also, one expects significant changes in equilibrium bond distances in this cluster upon HAT implicating a role for significant inner-sphere reorganization contribution [34]. The features of relatively small E_a, small isotope effect, and small rate constant (from a small A factor) emerge from the HAT theory for the bonded framework model, with some involvement of inner-sphere vibrations.

3. Proton transfer in cytochrome *c* oxidase

Proton translocation shares features in common with charge transfer reactions. Consider a chain of hydrogen bonded water molecules with an excess proton added to one end of the chain. The Grotthuss [35] mechanism suggests that the hydrogen bonds linking successive oxygens can "flip" and deliver the excess proton to the other end of the chain, without a requirement of (slow) mass transport. For each successive heavy atom pair, a proton tunnels through its potential surface. We have commenced an analysis of proton transfer and translocation in CcO based on this idea, which is quite similar in spirit to the above discussion of PCET and HAT reactions. It uses a combination of quantum mechanics (QM) for the protons that can transfer, and molecular dynamics (MD) for the heavy atom degrees of freedom. Once again, use of the Born–Oppenheimer separation permits construction of light particle potential surfaces parametric on the surrounding medium's configuration. For a given surface, we solve the Schrödinger equation to obtain the protons' wave functions—they will almost always be localized either in their respective initial or transferred states. With the protons' probability distributions (wave functions squared) and the conventional MD forces, the state of the system can be updated by an MD step. This new heavy-atom configuration provides a new potential surface for the protons, and the Schrödinger equation is solved again. If this scheme is iterated sufficiently, an account of proton transfer and translocation driven by medium thermal fluctuations can be given. The methodology is analogous to what has been used previously to discuss electron localization in liquids [36–39].

The QM/MD procedure is carried out using CUKMODY [40], an MD program that we designed for protein MD in such a way as to readily interface with quantum calculations exemplified by the proton transfer/translocation process discussed above. The MD uses the GROMOS [41] force-field suitably modified to account for type *a* hemes, and the various metals found in CcO. The starting configuration was obtained from a preliminary version [42] of the recently published X-ray crystal structure of cytochrome *c* oxidase from *Rhodobacter sphaeroides* [43]. Only subunits I and II were included in the simulation. After removing waters that overlap with the protein, there were 18,399 water molecules left in the simulation box. Hydrogen bonded chains that form from waters and residues are critical to this discussion. We designed an algorithm to search for sites to place waters in the crystal structure [40]. Roughly 500 are inside the protein by our construction.

After 650 ps of just MD, we observe a cyclic structure formed by two hydrogen bonded waters that are each

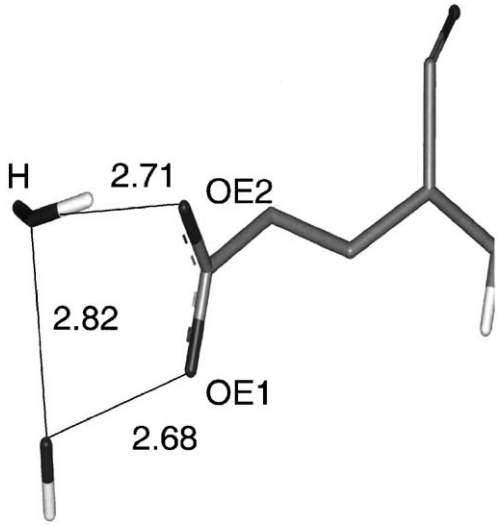

Fig. 3. Two hydrogen bonded waters that are hydrogen bonded to, respectively, the OE1 and the OE2 of the carboxylate group of Glu286. The proton that forms the hydrogen bond between the two waters and the water proton that is hydrogen bonded to OE1 are *not* displayed, since they will be treated as wave functions. An excess proton has been added to the water hydrogen bonded to OE1, forming the cycle $H_5O_2^+$-Glu. The geometry indicates that all three hydrogen bonds are strong, and the structure is quite persistent in time. This configuration is used as the starting point for the QM/MD simulation.

hydrogen bonded to the carboxylate oxygens of Glutamate 286, as shown in Fig. 3. In *R. sphaeroides*, this glutamate, which is positioned close to the a_3 heme in the D-pathway [44,45] that originates at Asp132 (close to the cytoplasmic side of the bacterial membrane), has been suggested to play an important role in proton translocation [43,46–53]. The two protons that are considered for transfer are *not* displayed since they will be treated as wave functions. The waters have migrated to their positions during the course of the simulation. At this point, we attach an excess proton to the water that hydrogen bonds to OE2 (cf. Fig. 3) and, from here, we start the QM/MD, solving for the wave functions of both protons. Note that the pes for the two protons consists of two terms: a gas phase ab initio surface, which has an assumption about the strength of the stabilization of the proton to the glutamate OE1, and the solvation from the surrounding protein, cofactors and waters. A 100-ps time record of each proton's expectation value, $\langle x\rangle(t)$, is displayed in Fig. 4. The second proton's $\langle x\rangle(t)$ (the one that can transfer to protonate the glutamate) is displaced by one Angstrom for clarity. That is, the first (second) proton's $\langle x\rangle(t)$ in its initial state is centered around 1.0 (2.0) Å and, when transferred, the first (second) proton's $\langle x\rangle(t)$ is centered around 1.8 (2.8) Å. It is clear that both protons are hopping back and forth between their respective surrounding oxygen atoms, and they do so in a correlated fashion. Importantly, the protonic hop time is on a several-femtosecond time scale. The origin of this hopping time scale is that it only takes on the order of a 1 kcal/mol "asymmetry" (the energy difference between the minima of the double well pes for a given proton being in its final and initial states) to localize the proton on the lower energy side. Since the dynamics of the solvent thermal fluctuations can produce a 1 kcal/mol asymmetry in a few (2 fs) MD time steps, the solvation contribution can switch which state is stable on this time scale. In Fig. 4, the protons spend more time in their respective transferred states because we have made the second proton's transfer to the glutamate 12 kcal/mol exoergic, by construction of the ab initio surface. When the ab initio proton surface is thermoneutral, both protons hop back and forth on this rapid time scale and, on average, spend close to equal time in their possible states, indicating that there is no great asymmetry in the solvation they experience. Note that the proton hop time reflects the kinetic barrier to proton transfer and does not correlate with the length of time a proton spends in its possible states. The quantity that can be related to an equilibrium constant is the total dwell time in each proton state. Thus, by counting the dwell time in the two states, a $\Delta pK_a \equiv pK_a - pH$ value can be inferred. For the data shown, the ΔpK_a of Glu286 is 1.67. A potential surface for this system is not available directly; however, the pK_as of glutamates in various environments are known and tend to be increased, relative to its standard value, in protein active sites [54,55]. Indeed, there is spectroscopic evidence for protonation of Glu286 at neutral pH, with an estimated pK_a of 8–9 [46,47].

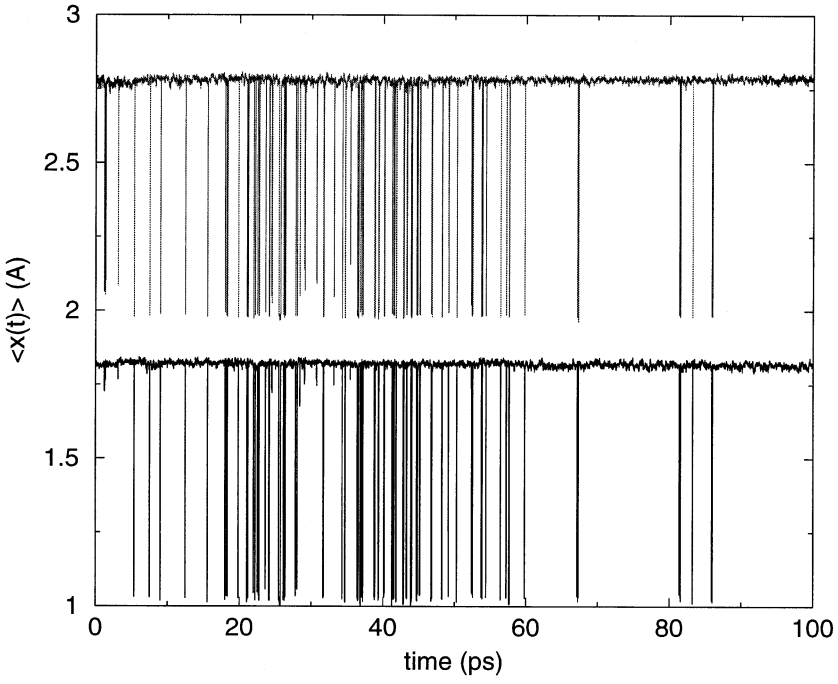

Fig. 4. The time-dependent expectation value, $\langle x\rangle(t)$, of each quantum proton's position. The data for proton 2 is displaced by +1 Å for clarity of presentation. The second proton's $\langle x\rangle(t) \sim 2.8$ indicates the protonation of Glu286's OE1. The gas-phase surface for the second proton's transfer to OE1 of the glutamate was chosen as exoergic, favoring protonation of Glu. The solvation component could counteract this but does not.

In our view, knowing what fraction of time a proton spends protonating a particular residue is operationally useful. If there is sufficient averaging time to sample a broad range of solvent fluctuations, then the relative dwell time can be associated with an equilibrium constant and a ΔpK_a value. Note, however, that a thermodynamic, equilibrium property is not a useful concept here; only a transient, local equilibrium should be inferred from such simulations. Obviously, a proton hopping back and forth indefinitely will not lead to proton translocation. What must happen is that a longer-time-scale protein rearrangement will, e.g., induce a now protonated glutamate to release the proton to another water/residue and continue the translocation process. In order to explore such a scenario, we have designed a tree-search-based algorithm [40] that can find pathways of arbitrarily long chains of hydrogen bonded water molecules that can span various regions of the protein.

One such pathway of interest could stretch from the Glu286 to the Magnesium ion, as it could serve to provide a hydrogen bonded chain of waters and/or residues capable of a Grotthuss translocation mechanism carrying protons toward the outside. In Fig. 5 we display just such a chain that has formed after about 3 ns of run time. The figure is oriented with the cytoplasmic (inner) side of the membrane down with the D-pathway running from the bottom up to Glu286. One water is hydrogen bonded to the Glu286 carboxylate and it is connected by a continuous chain of hydrogen bonded waters to a water that is hydrogen bonded to the Mg^{2+}. We find that such transient chains form and reform constantly and can provide a number of different pathways between Glu286 and the Magnesium ion. Similar chains are found for the simulations that we start by using Glu286 when protonated as a starting configuration and running MD from this configuration. Water chains related to those found in this work have been discussed by Zheng et al. [56].

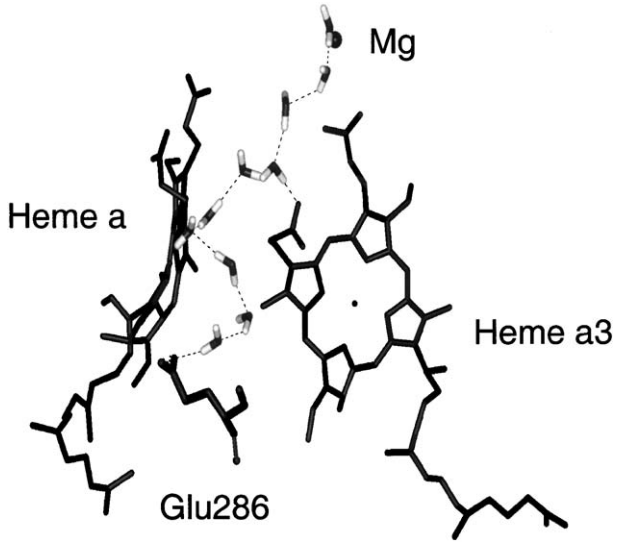

Fig. 5. A chain of hydrogen bonded waters that have formed spanning Glu286 to Mg^{2+}. The orientation has the cytoplasmic (inner) side at the bottom with the D-pathway pointing up to Glu286. One end of the chain has a water hydrogen bonded to the Glu286 carboxylate and the other end has a water hydrogen bonded to Mg^{2+}. Also displayed are the two hemes, heme *a* and heme a_3. The hydrogen bond between a water and the carboxylate of the heme a_3 D-propionate is quite persistent. This snapshot is at a time around 3 ns after the beginning of the MD run.

Missing from our current simulations on translocation is the role of the oxidation state of the system in influencing the proton translocation properties. The role of the coupling between electron transfer and proton translocation is analogous to that in the PCET problems discussed above and, in principle, is also amenable to the QM/MD simulation methods just outlined.

Acknowledgements

The financial support of the National Institutes of Health (GM 47274) is gratefully acknowledged.

References

[1] C. Tommos, G.T. Babcock, Proton and hydrogen currents in photosynthetic water oxidation, Biochim. Biophys. Acta 1458 (2000) 199–219.
[2] S. Ferguson-Miller, G.T. Babcock, Heme/copper terminal oxidases, Chem. Rev. 96 (1996) 2889–2908.
[3] K.L. Westphal, C. Tommos, R.I. Cukier, G.T. Babcock, Concerted hydrogen-atom abstraction in photosynthetic water oxidation, Curr. Opin. Plant Biol. 3 (2000) 236–242.
[4] K.L. Westphal, N. Lydakis-Simantiris, R.I. Cukier, G.T. Babcock, Effects of Sr^{2+} substitution on the reduction rates of Y_Z in PSII membranes—evidence for concerted hydrogen-atom transfer in oxygen evolution, Biochemistry 39 (2000) 16220–16229.
[5] R. Cukier, D. Nocera, Proton-coupled electron transfer, Annu. Rev. Phys. Chem. 49 (1998) 337–369.
[6] R.I. Cukier, in: R.A. Wheeler (Ed.), Bioenergetics Simulations of Electron, Proton, and Energy Transfer, American Chemical Society Symposium Series, 2003, p. 194.
[7] C.W. Hoganson, G.T. Babcock, A metalloradical mechanism for the generation of oxygen from water in photosynthesis, Science 277 (1997) 1953–1956.
[8] C. Tommos, G.T. Babcock, Oxygen production in nature: a light-driven metalloradical enzyme process, Acc. Chem. Res. 31 1998, pp. 18–25.
[9] B. Meyer, E. Scholddr, J.P. Dekker, H.T. Witt, O_2 evolution and Chl a^+(P-680$^+$) nanosecond reduction kinetics in single flashes as a function of pH, Biochim. Biophys. Acta 974 (1989) 36–43.
[10] C. Tommos, X.-S. Tang, K. Warncke, C.W. Hoganson, S. Styring, J. McCracken, B.A. Diner, G.T. Babcock, Spin-density distribution, conformation, and hydrogen bonding of the redox-active tyrosine Y_Z in photosystem II from multiple electron magnetic-resonance spectroscopies: implications for photosynthetic oxygen evolution, J. Am. Chem. Soc. 117 (1995) 10325–10335.
[11] H.-A. Chu, A.P. Nguyen, R. Debus, Amino acid residues that influence the binding of manganese or calcium to photosystem II: 1. The lumenal interhelical domains of the D1 polypeptide, Biochemistry 34 (1995) 5839–5858.
[12] C.F. Yocum, V.L. Pecoraro, Recent advances in the understanding of

the biological chemistry of manganese, Curr. Opin. Struct. Biol. 3 (1999) 182–187.
[13] J. Barber, W. Kuhlbrandt, Photosystem II, Curr. Opin. Struct. Biol. 9 (1999) 469–475.
[14] J. Ulstrup, Charge Transfer Processes in Condensed Media, Springer, Berlin, 1979.
[15] B. Fain, Lecture Notes in Chemistry: Theory of Rate Processes in Condensed Media, Springer-Verlag, Berlin/Heidelberg, 1980.
[16] L.I. Krishtalik, Charge Transfer Reactions in Electrochemical and Chemical Processes, Plenum, New York, 1979.
[17] R.I. Cukier, A theory that connects proton-coupled electron-transfer and hydrogen-atom transfer reactions, J. Phys. Chem., B 106 (2002) 1746–1757.
[18] V.G. Levich, R.R. Dogonadze, E.D. German, A.M. Kuznetsov, Y.I. Kharkats, Theory of homogeneous reactions involving proton transfer, Electrochim. Acta 15 (1970) 353–367.
[19] A.M. Kuznetsov, J. Ulstrup, Proton and hydrogen atom tunnelling in hydrolytic and redox enzyme catalysis, Can. J. Chem. 77 (1999) 1085–1096.
[20] D. Borgis, A. Staib, Quantum adiabatic umbrella sampling: the excited state free energy surface of an electron-atom pair in solution, J. Chem. Phys. 104 (1996) 4776–4783.
[21] R.I. Cukier, J. Zhu, Simulation of proton transfer reaction rates: the role of solvent electronic polarization, J. Phys. Chem. 101 (1997) 7180–7190.
[22] H. Decornez, S. Hammes-Schiffer, Model proton-coupled electron transfer reactions in solution: predictions of rates, mechanisms, and kinetic isotope effects, J. Phys. Chem., A 104 (2000) 9370–9384.
[23] N. Iordanova, H. Decornez, S. Hammes-Schiffer, Theoretical study of electron, proton, and proton-coupled electron transfer in iron bi-imidazoline complexes, J. Am. Chem. Soc. 123 (2001) 3723–3733.
[24] Y. Georgievskii, A.A. Stuchebrukhov, Concerted electron and proton transfer: transition from nonadiabatic to adiabatic proton tunneling, J. Chem. Phys. 113 (2000) 10438–10450.
[25] E.E. Nikitin, S.Y. Umanskii, Theory of Slow Atomic Collisions, Springer-Verlag, Berlin, 1984.
[26] R.P. Bell, The Tunnel Effect in Chemistry, Chapman & Hall, London, 1980.
[27] C. Tommos, C.W. Hoganson, M. DiValentin, N. Lydakis-Simantiris, P. Dorlet, K. Westphal, H.-A. Chu, J. McCracken, G.T. Babcock, Manganese and tyrosyl radical function in photosynthetic oxygen evolution, Curr. Opin. Chem. Biol. 2 (1998) 244–252.
[28] M. Karge, K.D. Irrgang, G. Renger, Analysis of the reaction coordinate of photosynthetic water oxidation by kinetic measurements of 355 nm absorption changes at different temperatures in Photosystem II preparations suspended in either H2O or D2O, Biochemistry 36 (1997) 8904–8913.
[29] P. Dorlet, M. DiValentin, G.T. Babcock, J.L. McCracken, Interaction of $Y_Z^{\bullet}$ with its environment in acetate-treated Photosystem II membranes and reaction center cores, J. Phys. Chem., B 102 (1998) 8239–8247.
[30] J.M. Peloquin, K.A. Campbell, R.D. Britt, 55Mn pulsed ENDOR demonstrates that the Photsystem II "split" EPR signal arises from a magnetically-coupled mangano-tyrosyl complex, J. Am. Chem. Soc. 120 (1998) 6840–6841.
[31] K.V. Lakshmi, S.S. Eaton, G.R. Eaton, H.A. Frank, G.W. Brudvig, Analysis of dipolar and exchange interactions between manganese and tyrosine Z in the S2YZ state of acetate-inhibited Photosystem II via EPR spectral simulations at X- and Q-bands, J. Phys. Chem., B 102 (1998) 8327–8335.
[32] A. Zouni, H.T. Witt, J. Kern, P. Fromme, N. Krauss, W. Saenger, P. Orth, Crystal structure of photosystem II from *Synechococcus elongatus* at 3.8 angstrom resolution, Nature 409 (2001) 739–743.
[33] N. Kamiya, J.R. Shen, Crystal structure of oxygen-evolving photosystem II from *Thermosynechococcus vulcanus* at 3.7-angstrom resolution, Proc. Natl. Acad. Sci. U. S. A. 100 (2003) 98–103.
[34] M.R.A. Blomberg, P.E.M. Siegbahn, S. Styring, G.T. Babcock, B. Åkermark, P. Korall, A quantum chemical study of hydrogen abstraction from manganese coordinated water by a tyrosyl radical: a model for water oxidation in Photosystem II, J. Am. Chem. Soc. 119 (1997) 8285–8292.
[35] J.F. Nagle, S. Tristam-Nagle, Hydrogen bonded chain mechanisms for proton conduction and proton pumping, J. Membr. Biol. 74 (1983) 1–14.
[36] A. Selloni, P. Carnevali, R. Car, M. Parrinello, Localization, hopping, and diffusion of electrons in molten salts, Phys. Rev. Lett. 59 (1987) 823–826.
[37] R.N. Barnett, U. Landman, A. Nitzan, Dynamics and spectra of a solvated electron in water clusters, J. Chem. Phys. 89 (1988) 2242–2256.
[38] P.J. Rossky, J. Schnitker, The hydrated electron: quantum simulation of structure, spectroscopy, and dynamics, J. Phys. Chem. 92 (1988) 4277–4285.
[39] J. Zhu, R.I. Cukier, A quantum molecular dynamics simulation of an excess electron in methanol, J. Chem. Phys. 98 (1993) 5679–5693.
[40] R.I. Cukier, S.A. Seibold, Molecular dynamics simulations of prostaglandin endoperoxide II synthase-1: role of water and the mechanism of compound I formation from hydrogen peroxide, J. Phys. Chem., B 106 (2002) 12031–12044.
[41] W.F. van Gunsteren, H.J.C. Berendsen, GROMOS Manual, Groningen University, Groningen, 1987.
[42] S. Ferguson-Miller (2003). Coordinates kindly provided by Professor S. Ferguson-Miller.
[43] M. Svensson-Ek, J. Abramson, G. Larsson, S. Tornroth, P. Brzezinski, S. Iwata, The X-ray crystal structures of wild-type and EQ(I-286) mutant cytochrome *c* oxidases from *Rhodobacter sphaeroides*, J. Mol. Biol. 321 (2002) 329–339.
[44] S. Yoshikawa, K. Shinzawa-Itoh, R. Nakashima, R. Yaono, E. Yamashita, N. Inoue, M. Yao, M.J. Fei, C.P. Libeu, T. Mizushima, H. Yamaguchi, T. Tomizaki, T. Tsukihara, Redox-coupled crystal structural changes in bovine heart cytochrome *c* oxidase, Science 280 (1998) 1723–1729.
[45] S. Iwata, C. Ostermeier, B. Ludwig, H. Michel, Structure at 2.8-angstrom resolution of Cytochrome-C-Oxidase from *Paracoccus denitrificans*, Nature 376 (1995) 660–669.
[46] B. Rost, J. Behr, P. Hellwig, O.M.H. Richter, B. Ludwig, H. Michel, W. Mantele, Time-resolved FT-IR studies on the CO adduct of *Paracoccus denitrificans* cytochrome *c* oxidase: comparison of the fully reduced and the mixed valence form, Biochemistry 38 (1999) 7565–7571.
[47] A. Puustinen, J.A. Bailey, R.B. Dyer, S.L. Mecklenburg, M. Wikstrom, W.H. Woodruff, Fourier transform infrared evidence for connectivity between CuB and glutamic acid 286 in Cytochrome bo_3 from *Escherichia coli*, Biochemistry 36 (1997) 13195–13200.
[48] P. Adelroth, M. Svensson-Ek, D.M. Mitchell, R.B. Gennis, P. Brzezinski, Glutamate 286 in Cytochrome aa_3 from *Rhodobacter sphaeroides* is involved in proton uptake during the reaction of the fully reduced enzyme with dioxygen, Biochemistry 36 (1997) 13824–13829.
[49] B. Meunier, C. Ortwein, U. Brandt, P.R. Rich, Effects of mutation of residue 167 on redox-liinked protonation processes in yeast cytochrome *c* oxidase, Biochem. J. 330 1998, pp. 1197–1200.
[50] S. Junemann, B. Meunier, N. Fisher, P.R. Rich, Effects of mutation of the conserved glutamic acid-286 in subunit I of cytochrome *c* oxidase from *Rhodobacter sphaeroides*, Biochemistry 38 (1999) 5248–5255.
[51] C. Backgren, G. Hummer, M. Wikstrom, A. Puustinen, Proton translocation by cytochrome *c* oxidase can take place without the conserved glutamic acid in subunit I, Biochemistry 39 (2000) 7863–7867.
[52] A. Aagaard, G. Gilderson, D.A. Mills, S. Ferguson-Miller, P. Brzezinski, Redesign of the proton-pumping machinery of cytochrome *c* oxidase: proton pumping does not require Glu(I-286), Biochemistry 39 (2000) 15847–15850.

[53] P. Adelroth, M. Karpefors, G. Gilderson, F.L. Tomson, R.B. Gennis, P. Brzezinski, Proton transfer from glutamate 286 determines the transition rates between oxygen intermediates in cytochrome *c* oxidase, Biochim. Biophys. Acta 1459 (2000) 533–539.

[54] W.R. Forsyth, J.M. Antosiewiez, A.D. Robertson, Empirical relationships between protein structure and carboxyl pK(a) values in proteins, Proteins Struct. Funct. Genet. 48 (2002) 388–403.

[55] J.J. Dwyer, A.G. Gittis, D.A. Karp, E.E. Lattman, D.S. Spencer, W.E. Stites, B. Garcia-Morena E, High apparent dielectric constants in the interior of a protein reflect water penetration, Biophys. J. 79 (2000) 1610–1620.

[56] X. Zheng, D.M. Medvedev, J. Swanson, A.A. Stuchebrukhov, Computer simulation of water in cytochrome *c* oxidase, Biochim. Biophys. Acta 1557 (2003) 99–107.